

# Octocoral *Sarcophyton auritum* Verseveldt & Benayahu, 1978: Microanatomy and Presence of Collagen Fibers

Yael Mandelberg<sup>1</sup>, Dafna Benayahu<sup>2</sup>, and Yehuda Benayahu<sup>1,\*</sup>

<sup>1</sup>Department of Zoology, George S. Wise Faculty of Life Sciences, Tel Aviv University, Tel Aviv 69978, Israel; and <sup>2</sup>Cell and Developmental Biology, Sackler School of Medicine, Tel Aviv University, Tel Aviv 69978, Israel

**Abstract.** The study presents the microanatomy of the polyps of the reef-dwelling octocoral *Sarcophyton auritum*. We demonstrate the presence of its unique collagen fibers in the colony by means of Masson Trichrome histological staining. Based on peptide profiling, mass spectroscopy analysis confirmed that the fiber proteins were homologous with those of mammalian collagen. Histological and electron microscopy results showed that six of the eight mesenterial filaments of the polyps possess an internal, coiled, spring-like collagen fiber. High-resolution electron microscopy revealed for the first time in cnidarian collagen the interwoven, three-dimensional arrangement of the fibrils that comprise the fibers. Some fibrils feature free ends, while others are bifurcated, the latter being attributed to collagen undergoing fibrogenesis. Along with the mass spectroscopy finding, the coiled nature of the fibers and the fibril microanatomy show a resemblance to those of vertebrates, demonstrating the conserved nature of collagen fibers at both the biochemical and ultrastructural levels. The location, arrangement, and small diameter of the fibers and fibrils of *S. auritum* may provide a highly protective factor against occasional rupture and injury during the bending of the octocoral's extended polyps under strong current conditions; that is, providing the octocoral with a hydromechanical support. The findings from the microanatomical features of these unique fibers in *S. auritum*, as well as their suggested function, raise the potential for translation to biomedical applications.

## Introduction

Soft corals of the reef-dwelling genus *Sarcophyton* (Cnidaria, Octocorallia, Alcyonacea) are widespread, occurring

from the eastern coast of Africa and the Red Sea in the west to Polynesia in the east (Fabricius and Alderslade, 2001). The genus features about 52 species ([www.marinespecies.org/index.php](http://www.marinespecies.org/index.php)), which greatly contribute to the live cover on numerous coral reefs (*e.g.*, Verseveldt, 1982; Mandelberg-Aharon and Benayahu, 2015). *Sarcophyton* colonies possess a conspicuous stalk attached to the substrate, merging into a wider, fleshy, disc-like, polyp-bearing region termed the polypary. The polyps are dimorphic, featuring both autozooids and siphonozooids. Autozooids possess eight pinnate tentacles, which are completely retractile; siphonozooids are smaller in diameter, lack tentacles, and outnumber the autozooids (Fabricius and Alderslade, 2001). The polyps have the typical cnidarian structure of an external epidermis and an internal gastrodermis, which lines the polyp cavity (Fautin and Mariscal, 1991). Between these two cellular layers is the gelatinous coenenchyme—equivalent to the cnidarian mesoglea—containing thin-walled gastrodermal canals termed solenia, calcite sclerites, and some collagenous fibers (Fabricius and Alderslade, 2001).

Members of the phylum Cnidaria possess fibrillar and non-fibrillar collagenous proteins in their mesoglea. Their collagen is considered acellular, and is situated between the epidermal and gastrodermal cell layers (Tillet-Barret *et al.*, 1992). The mesoglea provides structural reinforcement and stiffness (*e.g.*, Gosline, 1971; Koehl, 1977; Thompson and Kier, 2001). In the different cnidarian classes, collagen acts as an extracellular matrix (ECM), providing scaffolding for cellular organization (*e.g.*, Tidball, 1982), and also playing a role in the skeletogenesis (*e.g.*, Ledger and Franc, 1978; Kingsley *et al.*, 1990) and functioning of nematocysts (*e.g.*, Brand *et al.*, 1993). In *Hydra* (class Hydrozoa), collagen characteristically features a thin ECM in the form of a basal membrane (Fowler *et al.*, 2000) and patterning polyp shape

Received 25 June 2015; accepted 4 December 2015.

\* To whom correspondence should be addressed. E-mail: yehudab@tauex.tau.ac.il

(Aufschnaiter *et al.*, 2011). The gelatinous mesogleal ECM of jellyfish (class Scyphozoa) exhibits a three-dimensional network of thin collagen fibrils (Gambini *et al.*, 2012). In the class Anthozoa, which includes sea anemones and corals, the mesoglea is of variable thickness, with thin, embedded collagen fibers that are thought to serve as reinforcing filler (Gosline, 1971). The collagen of octocorals has not been widely investigated; studies have examined the sea pen (Franc *et al.*, 1985; Tillet *et al.*, 1996) and the gorgonian (Kingsley *et al.*, 1990).

Our recent studies have shown that the octocoral *Sarcophyton ehrenbergi* (v. Marenzeller, 1886) exhibits unique, long collagen fibers, with highly reversible extensibility and rigidity, which are at the top of the reported range for mammalian collagen fibers (Benayahu *et al.*, 2013; Haj-Ali *et al.*, 2013; Sharabi *et al.*, 2014). The present study examined a congener, the Red Sea-endemic *Sarcophyton auritum* Verseveldt & Benayahu, 1983 (see also Mandelberg-Aharon and Benayahu, 2015), focusing on its unique fibers, which markedly differ from those previously reported for cnidarians. We sought to elucidate a) the microanatomy of the polyps and the position of collagen fibers in the colony, using specific histological staining; b) the protein composition of these fibers, with mass spectroscopy analysis; and c) the microstructure of the fibers, with electron microscopy. Because collagen has been a conserved protein throughout evolution (*e.g.*, Exposito *et al.*, 2008, 2010), it was intriguing to examine these newly-discovered collagen fibers. The understanding gained from these novel fibers is anticipated to contribute to implementation in practical biomedical applications (see also Haj-Ali *et al.*, 2013; Sharabi *et al.*, 2014, 2015).

## Materials and Methods

### Sample collection

To examine the microanatomy and collagen fibers in colonies of *Sarcophyton auritum*, samples measuring  $\sim 4 \times 3 \text{ cm}^3$  each were removed from the polypary of 8 colonies in the reef (3–5 m) across from the Interuniversity Institute for Marine Sciences in Eilat (IUI), Israel, northern Gulf of Aqaba (Red Sea) (February–August, 2012). Samples were individually placed in zip-lock bags underwater, then immediately brought to the laboratory for further processing. The collection of animals complied with a permit issued by the Israel Nature and National Parks Protection Authority.

### Microanatomy and histological studies

For histological study, small subsamples were taken from the larger samples, fixed overnight in 4% formaldehyde in seawater, rinsed with distilled water, and preserved in 70% ethyl alcohol. They were then decalcified for 2 successive

periods of 20 min each, using a mixture of formic acid and sodium citrate (Winsor, 1984), washed with distilled water, and dehydrated in a graded series of ethyl alcohol. The subsamples were placed in paraffin, and cross-sections measuring 6–7  $\mu\text{m}$  thick were obtained using a microtome (MIR; Shandon Lipshaw, Pittsburgh, PA). Histological slides were prepared with Masson Trichrome stain to visualize the collagen fibers (see Ross and Pawlina, 2006), then examined under a light microscope (Nikon Optiphot).

### Protein digestion and matrix-assisted laser desorption/ionization time of flight/time of flight (MALDI-TOF-TOF) analysis

Protein digestion and MALDI-TOF-TOF analysis were conducted. Upon collection, polypary subsamples of *Sarcophyton auritum* were immediately frozen at  $-20^\circ\text{C}$ , later defrosted, then placed on ice. To obtain isolated fibers, the material was ripped apart and the exposed fibers were carefully pulled out from the tissue using forceps. The fibers were washed in sterile, phosphate-buffered saline; any cellular debris was carefully removed under a dissecting microscope (Sharabi *et al.*, 2014).

The fibers were sonicated in a lysis buffer of 8 mol  $\text{l}^{-1}$  urea containing 400 mmol  $\text{l}^{-1}$  ammonium bicarbonate. Samples were reduced in 2.8 mmol  $\text{l}^{-1}$  DDT (1-dodecanethiol) at  $60^\circ\text{C}$  for 30 min, modified with 8.8 mmol  $\text{l}^{-1}$  iodoacetamide in 100 mmol  $\text{l}^{-1}$  ammonium bicarbonate in the dark at room temperature for 30 min, and digested overnight at  $37^\circ\text{C}$  in 2 mol  $\text{l}^{-1}$  urea and 25 mmol  $\text{l}^{-1}$  ammonium bicarbonate with modified trypsin (Promega Corp., Madison, WI) at a 1:50 enzyme-to-substrate ratio. The tryptic peptides were desalted using C18 tips (Harvard Apparatus, Cambridge, MA), dried, and resuspended in 0.1% formic acid. The peptide mixture was resolved by reverse-phase chromatography on  $0.075 \times 200\text{-mm}$ , fused silica capillaries (J&W Columns; Agilent Technologies, Santa Clara, CA) packed with Reprosil C18-Aqua (Dr. Maisch HPLC GmbH, Ammerbuch, Germany). The peptides were eluted with a 94-min linear gradient of 5%–28% solvent B (95% acetonitrile with 0.1% formic acid), and for 12 min at 95% acetonitrile with 0.1% formic acid in water at a flow rate of 0.15  $\mu\text{l}/\text{min}$ . Mass spectrometry (LTQ Orbitrap XL; Thermo Fisher Scientific, Waltham, MA) was performed in a positive mode using a repetitively full mass spectrometry (MS) scan, followed by collision-induced dissociation (CID; at 35 normalized collision energy) of the 7 most dominant ions ( $> 1$  charge) selected from the first MS scan. The mass spectrometry data were analyzed using Discoverer software version 1.3 (Thermo Fisher Scientific) and the Sequest search engine against the UniProt database for homologous proteins (UniProt Consortium, 2015). High

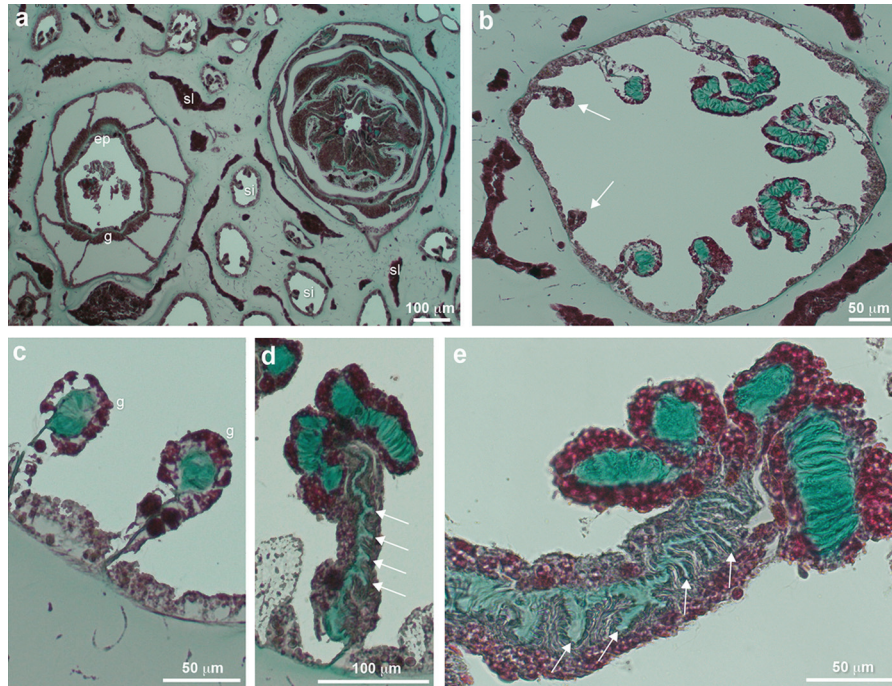


**Figure 1.** Light microscopy views of Masson Trichrome-stained cross-sections of *Sarcophyton auritum*, showing (a) an autozooid polyp at the pharyngeal level, with 8 mesenteries, the pharyngeal wall with thin mesoglea between the epidermis (ep) and gastrodermis (g), polyp retracted into the pharyngeal cavity, siphonozooids (si) with two short mesenteries, and solenia (sl). Among the autozooids, siphonozooids, and solenia is the light-turquoise-stained mesoglea. (b) Gastrovascular cavity with turquoise-stained collagen at the thickened edge of 6 mesenteries, and the other 2 mesenteries without this edge (arrows); (c) stained collagen in mesenterial filaments surrounded by gastrodermis (g) and mesentery, with thin mesoglea attached to the polyp body wall; (d) sections within a mesenterial filament showing the inner collagenous region of the mesentery, featuring asymmetrical extensions on one side (arrows); (e) magnified mesentery with 4 sections of convoluted mesenterial filament with inner fibrous collagen fiber; collagen in the mesentery featuring asymmetry: one side with remarkable, elongated extensions (arrows) and the other with none; gastrodermis is stained pinkish-red.

identifications were at a 1% false discovery rate (FDR), and medium identifications, at a 5% FDR.

#### *Scanning electron microscopy (SEM) and environmental scanning electron microscopy (ESEM)*

For SEM, subsamples were fixed in 4% glutaraldehyde in filtered seawater (0.22  $\mu\text{m}$  FSW), decalcified as described above, dehydrated through a graded series of ethanol up to 100%, and critical point dried with liquid  $\text{CO}_2$ . The preparations were fractured under a compound microscope, using the tips of fine forceps, and the gastrovascular cavities were then carefully exposed. They were next gold-coated and examined by SEM (JEOL JSM-840A SEM; JEOL Ltd., Tokyo, Japan). To obtain fiber preparations, fibers were isolated as described above, and stored in 70% ethanol. They were then processed, coated with gold palladium alloy, and examined at high vacuum by ESEM (JSM-6700 Field Emission Scanning Electron Microscope; JEOL Ltd.). Diameters of collagen fibers and fibrils were obtained from the images, using the ImageJ program (Schneider *et al.*, 2012).

#### *Transmission electron microscopy (TEM)*

For TEM, subsamples of the polypary were preserved in Karnovsky fixative (Karnovsky, 1965), decalcified, then washed with double-distilled water (DDW) and phosphate buffer. The subsamples were kept in 50% phosphate buffer and 50% Karnovsky fixative (Dykstra and Reuss, 2003), and embedded in Epon blocks (epoxy resin). Sections were obtained using a glass knife, stained with uranyl acetate and lead citrate, and examined by TEM (JEOL 1200EX; JEOL Ltd.).

## Results

#### *Microanatomy and histological studies*

Cross-sections of the *Sarcophyton auritum* polypary 2–3 mm below the surface featured a uniformly pale-turquoise-stained coenenchyme, found between the autozooids (hereafter termed “polyps”) and the siphonozooids (Fig. 1a). Histological sections of the polyps at the pharyngeal level exhibited eight mesenteries radiating from the inner polyp body wall across the gastrovascular cavity. This section was

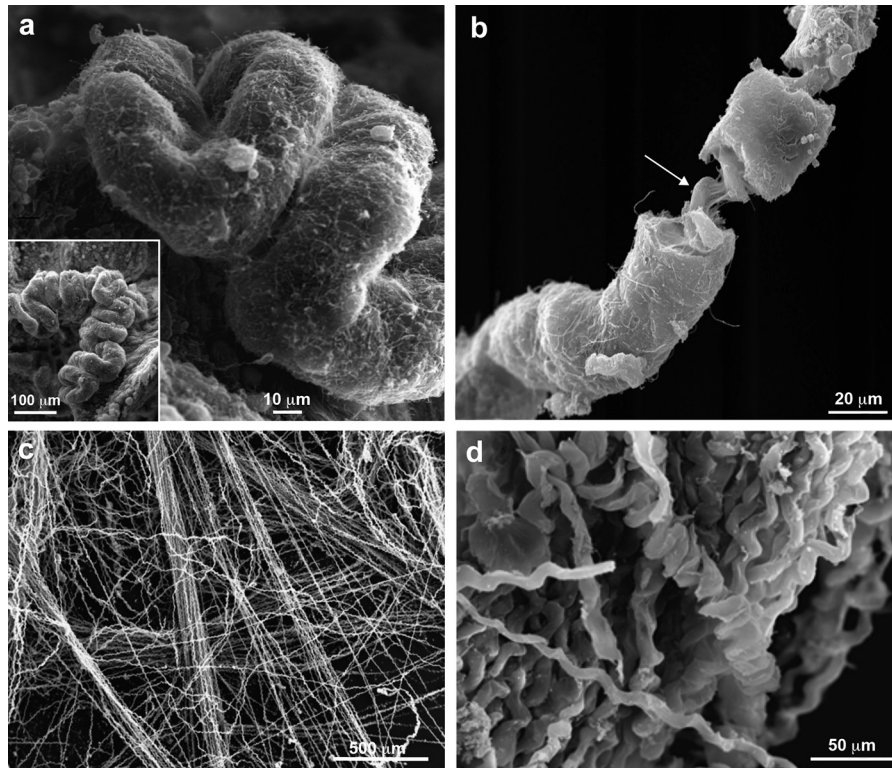


**Figure 2.** Scanning electron microscopy views of *Sarcophyton auritum*. (a) Mesenterial filament along the mesentery is convoluted (inset), tubular, with a ciliated surface. (b) Fractured, detached mesenterial filament revealing inner collagen fiber (arrow). (c) Extracted fibers featuring parallel and randomly oriented, coiled fibers. (d) Extracted fibers exhibiting various states of coiling.

turquoise from the Masson Trichrome stain, indicating the collagenous nature of the coenenchyme. A cross-section at the pharyngeal level of a retracted polyp similarly exhibited eight mesenteries. The coenenchyme featured sections of solenia and cross-sectioned siphonozooids, each of the latter bearing the characteristic two mesenteries (Fig. 1a). Figure 1b presents a cross-sectioned polyp below the pharynx, in which the edge of each of 6 radial mesenteries possesses a distinct, heavily turquoise-stained collagenous region. The remaining two short mesenteries of the polyp lack these turquoise-stained regions. The stained region corresponds to the polyp's mesenterial filament, which appears in the section as circular (Fig. 1b, c) or composite (Fig. 1b, d). The cross-sectioned edge of the mesentery demonstrates the convoluted nature of a contracted mesenterial filament (see Fig. 2); and, therefore, at a given plane, several sections might appear, each featuring turquoise-stained collagen surrounded by a dark-red-stained gastrodermis (Fig. 1d, e). The dark-turquoise-stained inner part of the mesenterial filament is comprised of a conspicuous fibrous collagen (Fig. 1d), unlike the uniformly stained coenenchyme (Fig. 1a–d). The cross-sectioned, inner collagenous part of the mesentery (Fig. 1d, e) is asymmetrical: only one side has clearly extended extensions, while the other side has none.

#### *Protein composition of fibers*

The histological cross-sections of *Sarcophyton auritum* (Fig. 1d, e) highlight the turquoise-stained inner part of the mesenterial filament, indicating the presence of fibrous collagen, surrounded by the endodermal cells. We isolated the fibers and analyzed their protein composition by liquid chromatography-mass spectrometry (LC-MS/MS). Proteome analysis characterized the organic matrices of the fibers; their tryptic cleavage led to the production of peptides that were separated by nano-liquid chromatography (nano-LC). The latter were then analyzed using tandem mass spectrometry (MS/MS) with an electrospray, high-resolution Mass Spectrometer-Orbitrap XL (Thermo Fisher Scientific). *In silico* analysis of the peptides confirmed the collagenous nature of the fibers as being mainly collagen type I. Since the database does not contain data from the *Sarcophyton auritum* proteome, the mass spectrometry data were analyzed against the Octocorallia and Cnidaria sections of the National Center for Biotechnology Information-Non-Redundant (NCBI-NR) database. The NCBI database contains only nine partially isolated proteins (<http://www.ncbi.nlm.nih.gov/protein/?term=Sarcophyton>). We then used the UniProt Knowledgebase (UniProt KB), which

**Table 1**

*Sarcophyton auritum*: protein identification of isolated fibers based on UniProt homology analysis

Accession number	Protein identification
P02453	Collagen alpha-1(I) chain = [CO1A1_BOVIN]
P04258	Collagen alpha-1(III) chain = [CO3A1_BOVIN]
P02465	Collagen alpha-2(I) chain = [CO1A2_BOVIN]
O46392	Collagen alpha-2(I) chain = [CO1A2_CANFA]
P85154	Collagen alpha-2(I) chain = [CO1A2_MAMAE]

is the central hub for functional information on proteins, with accurate, consistent, and rich annotation (UniProt Consortium, 2015). Consequently, we identified conserved peptides from other organisms, which enabled identification of the protein. The actual protein homology identification is presented in Table 1.

*Microstructure according to scanning (SEM), environmental (ESEM), and transmission (TEM) electron microscopy*

SEM images showed a convoluted mesenterial filament along the mesentery (Fig. 2a, inset), which was tubular, and which featured a ciliated surface (Fig. 2a). When the filament was detached from the mesentery and stretched, a fracture on its surface exposed an inner, coiled collagen fiber (Fig. 2b). Extracted collagen fibers commonly yielded bundles (Fig. 2c) with a coiled, spring-like organization (Fig. 2c, d). There were various coiling levels, with a pitch range of 6–40  $\mu\text{m}$ , most probably related to the force applied during their extraction from the polyps. The diameter size distribution of the fibers is presented in Figure 3a, and featured an average diameter of  $8.70 \pm 1.27 \mu\text{m}$  ( $n = 57$ ).

ESEM micrographs of the collagen fibers revealed their fibrillar composition (Fig. 4a). Higher magnification showed the 3-D arrangement of the fibrils, with an interwo-

ven organization within the coiled fiber (Fig. 4b). Some fibrils possessed bifurcated ends and others had free ends (Fig. 4c, d), suggesting that the fibrillogenesis process was taking place (see Discussion). The distribution of diameter size of the fibrils is presented in Figure 3b, showing an average diameter of  $23.72 \pm 3.05 \mu\text{m}$  ( $n = 45$ ).

TEM micrography of a cross-sectioned mesenterial filament yielded several sections of its collagen fiber at a given plane (Fig. 5a) embedded in the octocoral mesoglea, which also included some sections in the gastrodermis (Fig. 5b). An enlarged image of a sectioned fiber (Fig. 5c) shows longitudinal, striated fibrils typical of type I collagen and concentrically aligned, along with some cross-sectioned fibrils and longitudinal and oblique sectioned fibrils (Fig. 5d).

## Discussion

The microanatomical features of the polypary of the octocoral *Sarcophyton auritum* (Fig. 1) are presented. Overall, these features correspond to those known for other octocorals (Fabricius and Alderslade, 2001). However, our findings also revealed the unique microanatomical and ultrastructural characteristics of its mesenterial filaments, not previously documented for octocorals (Figs. 1 and 2). The distinctive microscopic and biochemical features of the fibrillar collagen of this species are provided, and shed new information on cnidarian collagen fibers. The fibers of *S. auritum* are situated in the mesenterial filaments, characteristically colored with Masson Trichrome stain (Fig. 1b–d and Fig. 2b), indicating their collagenous nature. This was also shown by proteomic analysis (Tables 1 and 2).

From basal metazoans, including cnidarians, to the highly specialized connective tissues of vertebrates, fibrillar collagens form a major structural element of the ECM (*e.g.*, Özbek *et al.*, 2010; Tucker *et al.*, 2011). Among cnidarians, the ECM has a variety of functions, but it mainly provides support for tissues, and it is the principal visible structure in

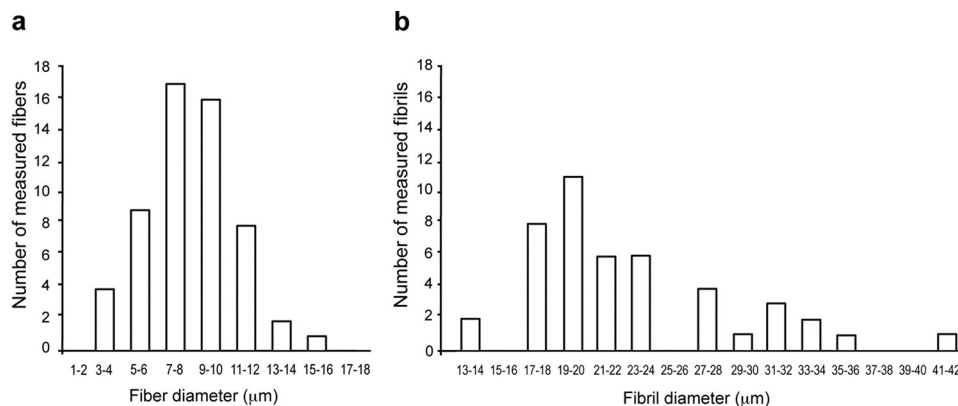


**Figure 3.** *Sarcophyton auritum*: (a) size frequency distribution of collagen fiber diameters; (b) size frequency distribution of fibril diameters.

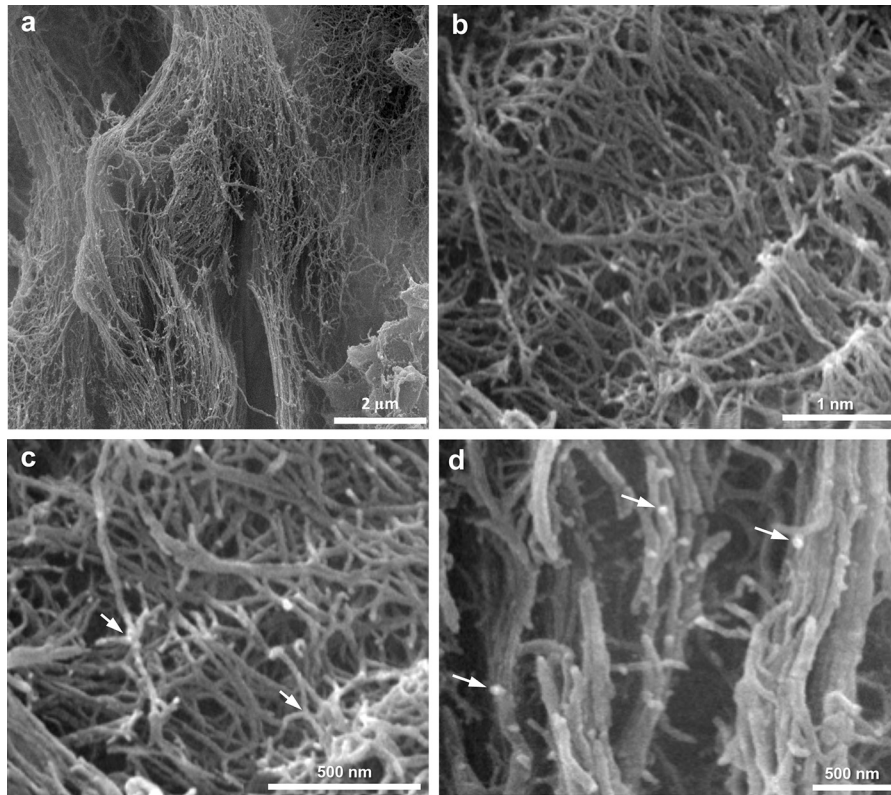


**Figure 4.** Environmental scanning electron microscopy views of *Sarcophyton auritum*. (a) Fibrillar composition of isolated fiber; (b) interwoven fibrils in a wavy arrangement; (c) bifurcated fibrils (arrows); and (d) free ends of fibrils (arrows).

the acellular mesoglea (e.g., Gosline, 1971; Chapman, 1974; Koehl, 1977; Tillet-Barret *et al.*, 1992). Little has changed in the perception of the structure of octocoral mesenterial filaments since the early work by Hyman (1940). The 2 filaments on the side opposite the siphonoglyph (the narrow, flagellated groove of the pharynx) are the longest and thickest, and are often bilobed; the filaments on the other 6 mesenteries contain digestive gland cells, and produce gonads (Fabricius and Alderslade, 2001). Mandelberg-Aharon and Benayahu (2015) demonstrated in *S. auritum* that these 6 mesenteries bear gonads that are similar to those of most other octocorals (Kahng *et al.*, 2011). The current findings render both *Sarcophyton auritum* and *Sarcophyton ehrenbergi* (see Benayahu *et al.*, 2013) unique among anthozoans in featuring distinct collagen fiber within their mesenterial filaments. In contrast, in Hexacorallia, the free edge of the mesenteries is expanded into unilobed or trilobed mesenterial filaments, which typically feature gland cells and cnidae (Daly *et al.*, 2003; Jahnel *et al.*, 2014). Their mesenteries contain longitudinal retractor muscle fibers, which aid in retraction and which have a hydrostatic function (Fautin and Mariscal, 1991; Jahnel *et al.*, 2014). Our results suggest that the mesenterial filaments of *S. auritum* provide a supportive structure that

differs from that found in hexacorals (collagen fibers vs. muscle fibers, respectively). Whether other congeners and other octocoral taxa share such features remains to be studied.

The current study highlights the microanatomy of *Sarcophyton auritum*, and, in particular, the position and unique ultrastructural features of its fibrillar collagen. The fibers are coiled, spring-like (Fig. 2b–d), and bear a resemblance to those of its congener *Sarcophyton ehrenbergi* (Sella, 2012; Benayahu *et al.*, 2013; Sharabi *et al.*, 2014). It is interesting to note that these fibers look a lot like the perimysial fibers found in the mammalian myocardium (e.g., Hanley *et al.*, 1999; Fleischer *et al.*, 2013), as supported by the microscopic, ultrastructural findings (Figs. 1–5). This observation supports the well-established notion that collagen is highly conserved among eukaryotes (e.g., Boot-Handford *et al.*, 2003; Özbek *et al.*, 2010), including the two phylogenetically remote groups (*i.e.*, cnidarians and mammals).

Figure 6 presents a schematic view of the polyp gastrovascular cavity of *S. auritum*, with collagen seen at the thickened edge of 6 mesenteries and an additional 2 mesenteries lacking such an edge. Figure 6 also depicts the convoluted mesenterial filaments, surrounded by gastrodermis and attached to the polyp body wall; the magnified inset shows a convoluted mesenterial filament with inner coiled collagen fiber.

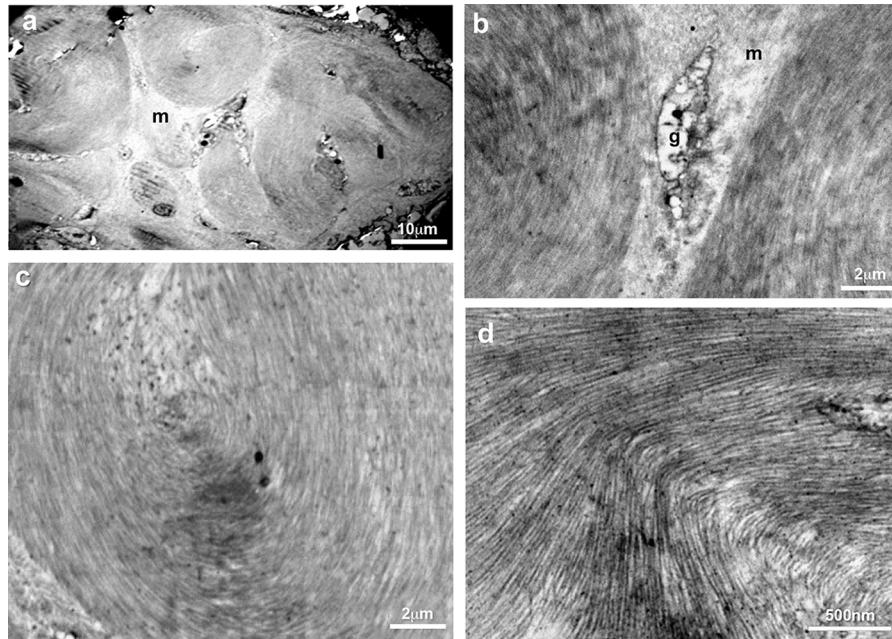


**Figure 5.** Transmission electron microscopy views of *Sarcophyton auritum*. (a) Cross-sectioned mesenterial filament with sections in coiled collagen fibers embedded in the mesoglea (m); (b) longitudinal sections of fibers revealing fibrils in a concentric arrangement, mesoglea (m), and gastrodermal insertion (g); (c) longitudinal section in fibrils; and (d) longitudinal and oblique sections in fibrils.

Isolated fibers demonstrated various pitch sizes, reflecting the degree of stretch from their native state within the mesentery, which occurred during the extraction procedure (Fig. 2b–d). They typically form fiber bundles comprised of coiled fibers (Sella, 2012; Fig. 2b–d). The diameter size range of *S. auritum* fibers and their mean are much lower (Fig. 3a) than the known 100–300- $\mu\text{m}$  range found, for example, in the rat tail tendon (Fratzl and Weinkamer, 2007). ESEM images revealed the interwoven, 3-D arrangement of the fibrils (Fig. 4a, b). These images show a fibril diameter (Fig. 3b) that falls within the lesser-known fibril range of 10–500 nm (*e.g.*, Parry and Craig, 1984; Tillet *et al.*, 1996). We suggest that the smaller-diameter size range of both fibers and fibrils of *S. auritum* acts as a highly protective factor against occasional rupture and injury during the bending of the extended polyps, as octocorals commonly experience strong currents in their natural coral-reef environment (Fabricius *et al.*, 1995; Y. Benayahu, pers. obs.). Undoubtedly, experimental monitoring of the fiber and fibrillar architecture as a response to mechanical stress will provide a better understanding of their adaptive significance.

The collagen fibril ends and bifurcations (Fig. 5b–d) suggest that fibrogenesis takes place within the mesenterial filament. For example, during this process in vertebrates, collagen fibrils have been shown to fuse together tip-to-tip, forming longer fibrils (Graham *et al.*, 2000). While bifurcations and fusions are observed both in normal tissue and

scar tissue, the bifurcations typically indicate the formation of new fibrils during the wound-healing process (*e.g.*, rat, Provenzano *et al.*, 2001; sheep, White *et al.*, 2002). In addition, early fetal development of the bovine and feline features fibrillar morphologies similar to those noted in our study (Provenzano and Vanderby, 2006). The high-resolution ESEM images obtained in the current study show, for the first time, the microstructural features of cnidarian collagen, highlighting their remarkable resemblance to the collagen of vertebrates, and displaying the conserved nature of the collagen at the ultrastructural level.

The TEM images of the mesenterial filaments also show the coiled nature of the fibers in their *in vivo* state within the mesenterial filament, as evidenced by the presence of several cross-sectioned fibers at a given plane (Fig. 5a, b). The mesoglea of *S. auritum* contains short, sparse collagen fibrils between the coiled fibers (Fig. 5b), as are commonly found in other cnidarians (*e.g.*, sea anemones, Singer, 1974; jellyfish, Gladfelter, 1972; and *Hydra*, Fowler *et al.*, 2000). The fibrils are also coiled, as evidenced by their concentric or oblique organization (Fig. 5b–d). These findings illustrate the hierarchical structure of the coiled fibers of *S. auritum*, which features fibers containing fibrils, yet which differs from a classical tendon, which also possesses aggregated fascicles that form the tendon (Fratzl and Weinkamer, 2007).

In summary, these microanatomical findings confirm, by histological staining, protein identification, and electron microscopy the collagenous nature of *Sarcophyton auritum*

**Table 2**

*Sarcophyton auritum*: peptide sequence retrieved for protein homology, as identified in Table 1

Accession number	Protein identification
P02453	<i>Collagen alpha-1(I) chain [CO1A1_BOVIN]</i> Peptide sequence GFSGLQGGPPGSPGEGQSPGASGPAGPR GANGAPGIAGAPGFPGAR GSAGPPGATGFPGAAGR GSPGEAGRPGEAGLPGAK GLTGSPGSPGPDGK TGPPGPAGQDGRPGPPGPPGAR GPPGPMGPPGLAGPPGESGR DGEAGAQQPPGPAGPAGER GDAGAPGAPGSQGAPGLQGMPPER GPSGPQGPSGPPGPK GEPGSPGENGAPQMGPGR GEPGPAGLPGPPGER DGLNGLPGPIGPPGPR
P04258	<i>Collagen alpha-1(III) chain [CO3A1_BOVIN]</i> Sequence DGASGHPGPIGPPGPR
P02465	<i>Collagen alpha-2(I) chain [CO1A2_BOVIN]</i> Peptide sequence GLPGVAGSVGEPGLGIAGPPGAR GEVGPAGPNGFAGPAGAAGQPGAKGER HGNRGEPPGAVGPAGAVGPR GAAGLPGVAGAPGLPGPR GDGGPPGATGFPGAAGR GLVGEPPGAGSK GPNGDSGRPGEPGLMGPGR
O46392	<i>Collagen alpha-2(I) chain [CO1A2_CANFA]</i> Peptide sequence GLPGVAGSVGEPGLGIAGPPGAR GDGGPPGATGFPGAAGR GEQGPAGPPGFQGLPGPAGTAGEVKGKPPER GLPGEFGLPGPAGPR GEVGPAGPNGFAGPAGAAGQPGAKGER GAAGLPGVAGAPGLPGPR GLPGEFGLPGPAGPR GIVGEPGAGSK GPNGDSGRPGEPGLMGPGR
P85154	<i>Collagen alpha-2(I) chain [CO1A2_MAMAE]</i> Peptide sequence GDGGPPGATGFPGAAGR TGETGASGPPGFAGEK GIPGEFGLPGPAGPR GAAGLPGVAGAPGLPGPR GIPGEFGLPGPAGPR GIVGEPGAGSK EGPAGLPGIDGRPGPIGPAGAR

fibers. These fibers are unique—compared to previously studied cnidarian fibers—in their position in the mesenterial filaments, their coiled nature, and their microstructural characteristics (Fig. 6). Their structural features may provide octocoral polyps with the ability to withstand the hydromechanical forces prevailing in the reef environment. Aufschnaiter *et al.* (2011) demonstrated that collagen is essen-

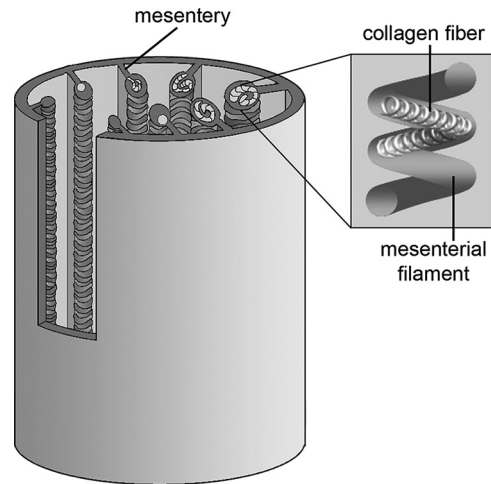


**Figure 6.** Schematic view of the gastrovascular cavity of a polyp of *Sarcophyton auritum*. Convoluted mesenterial filaments surrounded by gastrodermis are attached to the polyp body wall. Collagen is seen at the thickened edge of 6 mesenteries; the other 2 mesenteries lack this edge. Magnified inset features a convoluted mesenterial filament with inner, coiled collagen fiber.

tial for the structural patterning of *Hydra*; further research on octocorals along similar lines will undoubtedly bring to light more about the role of collagen. To better understand the functional adaptations of these fibers, future research should incorporate both *in vivo* and *in vitro* experimental studies, and examine the co-occurring microstructural changes at the fiber and fibrillar levels. Such studies will contribute to an understanding of the potential uses of these soft coral fibers for practical biomedical purposes.

### Acknowledgments

We thank The Interuniversity Institute for Marine Sciences in Eilat (IUI) for assistance and use of facilities. We are grateful to R. Haj-Ali and M. Sharabi for fruitful discussions and advice. We acknowledge M. Weis for assistance, Y. Delaria for SEM and TEM work, Z. Barkay for ESEM work, Y. Brickner and L. Maltz for histology work, E. Kaisler for photography, V. Wexler for digital editing, and N. Paz for editorial assistance. This research was supported in part by the endowment fund of the Israel Cohen Chair in Environmental Zoology (YB).

### Literature Cited

- Aufschnaiter, R., E. A. Zamir, C. D. Little, S. Özbek, S. Münder, C. N. David, L. Li, M. P. Sarras, Jr., and X. Zhang. 2011. *In vivo* imaging of basement membrane movement: ECM patterning shapes *Hydra* polyps. *J. Cell Sci.* **124**: 4027–4038.
- Benayahu, Y., D. Benayahu, Y. Kashman, A. Rudi, Y. Lanir, I. Sella, and E. Raz, inventors; Ramot at Tel Aviv University Ltd. (Tel Aviv, IL), assignee. 2013 Oct 8. Coral-derived collagen and methods of farming same. United States Patent No. 8,552,153.
- Boot-Handford, R. P., D. S. Tuckwell, D. A. Plumb, C. Farrington



- Rock, and R. Poulson. 2003.** A novel and highly conserved collagen (pro $\alpha$ 1(XVII)) with a unique expression pattern and unusual molecular characteristics establishes a new clade within the vertebrate fibrillar collagen family. *J. Biol. Chem.* **278**: 31067–31077.
- Brand, D. D., R. S. Blanquet, and M. A. Phelan. 1993.** Collagenaceous, thiol-containing proteins of cnidarian nematocysts: a comparison of the chemistry and protein distribution patterns in two types of cnidae. *Comp. Biochem. Physiol. Part B Comp. Biochem. Mol. Biol.* **106**: 115–124.
- Chapman, D. M. 1974.** Cnidarian histology. Pp. 2–36 in *Coelenterate Biology: Reviews and New Perspectives*, L. Muscatine, and H. M. Lenhoff, eds. Academic Press, New York.
- Daly, M., D. G. Fautin, and V. A. Cappola. 2003.** Systematics of the Hexacorallia (Cnidaria: Anthozoa). *Zool. J. Linn. Soc.* **139**: 419–437.
- Dykstra, M. J., and L. E. Reuss. 2003.** *Biological Electron Microscopy: Theory, Techniques and Troubleshooting*, 2nd ed. Springer US, New York.
- Exposito, J.-Y., C. Larroux, C. Cluzel, U. Valcourt, C. Lethias, and B. M. Degnan. 2008.** Demosponge and sea anemone fibrillar collagen diversity reveals the early emergence of A/C clades and the maintenance of the modular structure of Type V/XI collagens from sponge to human. *J. Biol. Chem.* **283**: 28226–28235.
- Exposito, J.-Y., U. Valcourt, C. Cluzel, and C. Lethias. 2010.** The fibrillar collagen family. *Int. J. Mol. Sci.* **11**: 407–426.
- Fabricius, K., and P. Alderslade. 2001.** *Soft Corals and Sea Fans: A Comprehensive Guide to the Tropical Shallow Water Genera of the Central-West Pacific, the Indian Ocean and the Red Sea*. Australian Institute of Marine Science, Townsville, Queensland, Australia.
- Fabricius, K. E., A. Genin, and Y. Benayahu. 1995.** Flow-dependent herbivory and growth in zooxanthellae-free soft corals. *Limnol. Oceanogr.* **40**: 1290–1301.
- Fautin, D. G., and R. N. Mariscal. 1991.** Cnidaria: anthozoa. Pp. 267–358 in *Microscopic Anatomy of Invertebrates*; Volume 2: *Placozoa, Porifera, Cnidaria, Ctenophora*, F. G. Harrison, J. A. Westfall, and A. Liss, eds. Wiley-Liss, New York.
- Fleischer, S., R. Feiner, A. Shapira, J. Ji, X. Sui, H. D. Wagner, and T. Dvir. 2013.** Spring-like fibers for cardiac tissue engineering. *Biomaterials* **34**: 8599–8606.
- Fowler, S. J., S. Jose, X. Zhang, R. Deutzmann, M. P. Sarras, Jr., and R. P. Boot-Handford. 2000.** Characterization of hydra type IV collagen. Type IV collagen is essential for head regeneration and its expression is up-regulated upon exposure to glucose. *J. Biol. Chem.* **275**: 39589–39599.
- Franc, S., P. W. Ledger, and R. Garrone. 1985.** Structural variability of collagen fibers in the calcareous axial rod of a sea pen. *J. Morphol.* **184**: 75–84.
- Fratzl, P., and R. Weinkamer. 2007.** Nature's hierarchical materials. *Prog. Mater. Sci.* **52**: 1263–1334.
- Gambini, C., B. Abou, A. Ponton, and A. J. M. Cornelissen. 2012.** Micro- and macrorheology of jellyfish extracellular matrix. *Biophys. J.* **102**: 1–9.
- Gladfelter, W. B. 1972.** Structure and function of the locomotory system of *Polyorchis montereyensis* (Cnidaria, Hydrozoa). *Helgol. Wiss. Meeresunters.* **23**: 38–79.
- Gosline, J. M. 1971.** Connective tissue mechanics of *Metridium senile*. *J. Exp. Biol.* **55**: 775–795.
- Graham, H. K., D. F. Holmes, R. B. Watson, and K. E. Kadler. 2000.** Identification of collagen fibril fusion during vertebrate tendon morphogenesis. The process relies on unipolar fibrils and is regulated by collagen-proteoglycan interaction. *J. Mol. Biol.* **295**: 891–902.
- Haj-ali, R., Y. Benayahu, D. Benayahu, A. Sason-Levi, and M. Sharabi. 2013 Aug 15.** Composites comprising collagen extracted from *Sarcophyton* sp. coral. United States Patent Application WO 2013118125 A1.
- Hanley, P. J., A. A. Young, I. J. LeGrice, S. G. Edgar, and D. S. Loisel. 1999.** 3-Dimensional configuration of perimysial collagen fibres in rat cardiac muscle at resting and extended sarcomere lengths. *J. Physiol.* **517**: 831–837.
- Hyman, L. H. 1940.** *The Invertebrates*. Vol. 1. *Protozoa Through Ctenophora*. McGraw-Hill, New York.
- Jahnel, S. M., M. Walzl, and U. Technau. 2014.** Development and epithelial organisation of muscle cells in the sea anemone *Nematostella vectensis*. *Front. Zool.* **11**: 44.
- Kahng, S. E., Y. Benayahu, and H. Lasker. 2011.** Sexual reproduction in octocoral. *Mar. Ecol. Prog. Ser.* **443**: 265–283.
- Karnovsky, M. J. 1965.** A formaldehyde-glutaraldehyde fixative of high osmolality for use in electron microscopy [Abstract]. *J. Cell Biol.* **27**: 137–8A.
- Kingsley, R. J., M. Tsuzaki, N. Watabe, and G. L. Mechanic. 1990.** Collagen in the spicule organic matrix of the Gorgonian *Leptogorgia virgulata*. *Biol. Bull.* **179**: 207–213.
- Koehl, M. A. R. 1977.** Mechanical diversity of the connective tissue of the body wall of sea anemones. *J. Exp. Biol.* **69**: 107–125.
- Ledger, P. W., and S. Franc. 1978.** Calcification of the collagenous axial skeleton of *Veretillum cynomorium* pall. (Cnidaria: Pennatulacea). *Cell Tissue Res.* **192**: 249–266.
- Mandelberg-Aharon, Y., and Y. Benayahu. 2015.** Reproductive features of the Red Sea octocoral *Sarcophyton auritum* Verseveldt & Benayahu, 1978 are uniform within generic boundaries across wide biogeographical regions. *Hydrobiologia* **759**: 119–132.
- Özbek, S., P. G. Balasubramanian, R. Chiquet-Ehrismann, R. P. Tucker, and J. C. Adams. 2010.** The evolution of extracellular matrix. *Mol. Biol. Cell.* **21**: 4300–4305.
- Parry, D. A. D., and A. S. Craig. 1984.** Growth and development of collagen fibrils in connective tissue. Pp. 34–64 in *Ultrastructure of the Connective Tissue Matrix*, Electron Microscopy in Biology and Medicine 3, A. Ruggeri, and P. M. Motte, eds. Springer US, New York.
- Provenzano, P. P., and R. Vanderby, Jr. 2006.** Collagen fibril morphology and organization: implications for force transmission in ligament and tendon. *Matrix Biol.* **25**: 71–84.
- Provenzano, P. P., C. Hurschler, and R. Vanderby, Jr. 2001.** Microstructural morphology in the transition region between scar and intact residual segments of a healing rat medial collateral ligament. *Connect. Tissue Res.* **42**: 123–133.
- Ross, M. H., and W. Pawlina. 2006.** *Histology: a Text and Atlas: with Correlated Cell and Molecular Biology*, 5<sup>th</sup> ed. Lippincott Williams & Wilkins, Baltimore.
- Schneider, C. A., W. S. Rasband, and K. W. Eliceiri. 2012.** NIH Image to ImageJ: 25 years of image analysis. *Nat. Methods* **9**: 671–675.
- Sella, I. 2012.** Biological, biochemical, and mechanical properties of collagen fibers of the soft coral *Sarcophyton ehrenbergi*. Ph.D. dissertation, Tel-Aviv University.
- Sharabi, M., Y. Mandelberg, D. Benayahu, Y. Benayahu, A. Azem, and R. Haj-Ali. 2014.** A new class of bio-composite materials of unique collagen fibers. *J. Mech. Behav. Biomed. Mater.* **36**: 71–81.
- Sharabi, M., D. Benayahu, Y. Benayahu, J. Isaacs, and R. Haj-Ali. 2015.** Laminated collagen-fiber bio-composites for soft-tissue biomimetics. *Compos. Sci. Technol.* **117**: 268–276.
- Singer, I. I. 1974.** An electron microscopic and autoradiographic study of mesogleal organization and collagen synthesis in the sea anemone *Aiptasia diaphana*. *Cell Tissue Res.* **149**: 537–554.
- Thompson, J. T., and W. M. Kier. 2001.** Ontogenetic changes in fibrous connective tissue organization in the oval squid, *Sepioteuthis lessoniana* Lesson, 1830. *Biol. Bull.* **201**: 136–153.
- Tidball, J. G. 1982.** An ultrastructural and cytochemical analysis of the cellular basis for tyrosine-derived collagen crosslinks in *Leptogorgia virgulata* (Cnidaria: Gorgonacea). *Cell Tissue Res.* **222**: 635–645.

- Tillet, E., J.-M. Franc, S. Franc, and R. Garrone. 1996.** The evolution of fibrillar collagens: a sea-pen collagen shares common features with vertebrate type V collagen. *Comp. Biochem. Physiol. B Biochem. Mol. Biol.* **113**: 239–246.
- Tillet-Barret, E., J.-M. Franc, S. Franc, and R. Garrone. 1992.** Characterization of heterotrimeric collagen molecules in a sea pen (Cnidaria, Octocorallia). *Eur. J. Biochem.* **203**: 179–184.
- Tucker, R. P., B. Shibata, and T. N. Blankenship. 2011.** Ultrastructure of the mesoglea of the sea anemone *Nematostella vectensis* (Edwardsiidae). *Invertebr. Biol.* **130**: 11–24.
- UniProt Consortium. 2015.** UniProt: a hub for protein information. *Nucl. Acids Res.* **43**: D204–D212.
- Verveeldt, J. 1982.** A revision of the genus *Sarcophyton* Lesson (Octocorallia, Alcyonacea). *Zool. Verh. Leiden* **192**: 1–91.
- White, J. F., J. A. Werkmeister, I. A. Darby, T. Bisucci, D. E. Birk, and J. A. M. Ramshaw. 2002.** Collagen fibril formation in a wound healing model. *J. Struct. Biol.* **137**: 23–30.
- Winsor, L., compiler. 1984.** *Manual of Basic Zoological Microtechniques for Light Microscopy*. School of Biological Sciences, James Cook University of North Queensland, Townsville, Australia.